Numerical analysis of cone penetration testing in anisotropic clayey materials

Diego Durán[12#], *Lluís* Monforte[2], *Marcos* Arroyo[1,2] and *Antonio* Gens[1,2]

[1]*Universitat Politècnica de Catalunya (UPC)*
Campus Nord UPC, Carrer Jordi Girona, 1-3, Edifici D2, 08034 Barcelona, Spain

[2]*Centre Internacional de Mètodes Numèrics en Enginyeria (CIMNE)*
Campus Nord UPC, Carrer Jordi Girona, 1-3, Edifici C1, 08034 Barcelona, Spain

[#]*Corresponding author: diego.duran.caballero@upc.edu*

ABSTRACT

Most natural clays acquire an anisotropic fabric upon deposition. This anisotropic fabric induces differences in the soil mechanical responses, for instance in the undrained shear strength observed in the laboratory. It is unclear how much of that anisotropy is reflected on the responses measured by the cone penetration test. In this work, we use GPFEM to numerically simulate cone penetration tests (CPTu) in undrained, anisotropic clays. The constitutive response is represented by S-CLAY1, a critical state, anisotropic model. Full details of the representative stress path during CPTu insertion are provided. Preliminary numerical results suggest that even a large amount of anisotropy, as described by the model, will have a very small effect on the cone responses. The numerical simulation results also show that the prevailing stress path has strong similitudes with that found during anisotropically-consolidated undrained compression triaxial test.

Keywords: CPTu; anisotropy; fabric; S-CLAY1; clays.

1. Introduction

The anisotropic behavior observed in natural soils is a consequence of the complex deposition processes and the stress history associated with soil sedimentation. These factors leave their imprint through anisotropic fabric features, giving raise to some internal oriented reference in the material. Anisotropic responses are then observed in the laboratory when performing the same test in differently oriented directions with respect to that internal reference. Mechanical anisotropy in soils is easy to observe at small strains by directed wave propagation (Arroyo & Muir Wood, 2003) but also when shearing at larger strains, for instance by applying the same stress path to specimens trimmed at different orientations from a block (e.g. Kirkgard & Lade, 1991). Observations of soil anisotropy at large strains are however complicated by the fact that the underlying anisotropic features evolve rapidly with applied strain.

Description and consideration of real soil anisotropy is sometimes complicated by the prevalence in practice of simplistic total-stress models, for which responses that do not necessarily reflect any material anisotropy appear as if anisotropic. A classic example of this pseudo-anisotropy is given by undrained shear strength, which is a coupled hydromechanical response that varies depending on the imposed loading condition or shearing modes. An isotropic effective stress model, formulated using stress invariants, predicts, for example, different values of undrained shear strength under triaxial compression and extension (Wood, 1990). In a total stress model, however, the same soil response will appear anisotropic.

The cone penetration tests with measurement of pore pressure (CPTu) is the most important in situ test for soft soils. Discussion of the effects of soil mechanical anisotropy on measured cone responses has generally focused on undrained penetration, such as that happening in clays. The ability to carry out realistic effective stress analyses of undrained cone penetration has been limited until recently. As a result, the discussion of anisotropic effects has often been framed using total stress models, (e.g. Su & Liao, 2002; Low et al. 2010; Su, 2010), which are not useful to distinguish the effect of real anisotropic behavior from pseudo-anisotropic responses.

To properly investigate the effect of clay anisotropic response on CPTu it is thus necessary to analyze undrained penetration using effective stress, to represent soil anisotropy and its evolution using an effective stress constitutive model and, finally, to represent cone insertion without imposing artificial symmetries in the problem, as it happens when cavity expansion models are employed. That was the approach taken by Moug et al. (2019), who employed an anisotropic effective stress formulation to represent cone insertion using FLAC. This is also the approach followed in this work.

In what follows, after reviewing the anisotropic constitutive model S-CLAY1 (Wheeler et al. 2003), we describe the effect of the initial fabric of the soil on the strength of the soil. Finally, we report a set of simulations of undrained CPTu testing, where full details of the shearing modes and stress path are given.

2. S-CLAY1

In this work, the constitutive response of the soil is modelled with S-CLAY1, a critical state, anisotropic constitutive model. For simplicity, the model is presented here for triaxial conditions and assuming a small strain formulation. The yield surface is a rotated ellipsoid in the p'- q plane:

$$f = (q - \alpha p')^2 - (M(\theta)^2 - \alpha^2)(p'_{\mathrm{m}} - p')p' = 0 \quad (1)$$

where $M(\theta)$ is stress ratio at critical state and depends on the Lode´s angle, θ. In this work, a smoothed Mohr-Coulomb surface is used to describe the relation between the stress ratio at critical state and the Lode angle. The soil fabric is represented by the scalar α and p'_{m} stands for the preconsolidation stress. The constitutive model includes two hardening laws:

- Volumetric hardening: the usual Modified Cam Clay (MCC) model expression describing the relation between volumetric plastic strains, $\varepsilon_{\mathrm{v}}^{\mathrm{p}}$, and the preconsolidation stress is employed:

$$\mathrm{d}p'_{\mathrm{m}} = \frac{v p'_{\mathrm{m}} \mathrm{d}\varepsilon_{\mathrm{v}}^{\mathrm{p}}}{\lambda - \kappa} \quad (2)$$

where v is the specific volume and λ and κ are the elastic compression and swelling slopes in the $v - ln\ p$ plane.

- Rotational hardening: describes the evolution of fabric due to plastic volumetric strains and plastic deviatoric strains; $\varepsilon_{\mathrm{d}}^{\mathrm{p}}$, and reads:

$$\mathrm{d}\alpha = \mu \left[\left(\frac{3\eta}{4} - \alpha \right) < \mathrm{d}\varepsilon_{\mathrm{v}}^{\mathrm{p}} > + \beta \left(\frac{\eta}{3} - \alpha \right) \left| \mathrm{d}\varepsilon_{\mathrm{d}}^{\mathrm{p}} \right| \right] \quad (3)$$

with μ and β being two parameters that control the rate of fabric creation and removal. Assuming an undrained response (as all simulations of this work do), a material that is continuously sheared, would have much lower volumetric plastic strains with respect to deviatoric plastic strains. Therefore, the fabric will asymptotically tend to $\alpha = \frac{M_\theta}{3}$ and the product $\mu\beta$ controls the rate at which the fabric approaches this asymptotic value.

The elastic model is assumed to be isotropic and the bulk and shear modulus are pressure dependent. Moreover, the same expression as in the MCC is employed. Thus, the elastic volumetric strain, $\varepsilon_{\mathrm{v}}^{\mathrm{e}}$, and elastic deviatoric strain, $\varepsilon_{\mathrm{d}}^{\mathrm{e}}$, and the mean effective stress and deviatoric strain invariant are related as:

$$\mathrm{d}\varepsilon_{\mathrm{v}}^{\mathrm{e}} = \frac{\kappa \mathrm{d}p'}{v p'} \qquad \mathrm{d}\varepsilon_{\mathrm{d}}^{\mathrm{e}} = \frac{\mathrm{d}q}{3G'} \quad (4)$$

where G' is the shear modulus of the soil and it can be calculated using a constant value of Poisson's ratio ν'.

As associated flow rule is assumed; therefore, the dilatancy rule (Wheeler et al. 2003) reads:

$$\frac{\mathrm{d}\varepsilon_{\mathrm{v}}^{\mathrm{p}}}{\mathrm{d}\varepsilon_{\mathrm{d}}^{\mathrm{p}}} = \frac{M^2 - \eta^2}{2(\eta - \alpha)} \quad (5)$$

The Modified Cam Clay model can be retrieved from the S-CLAY1 model by setting the initial fabric to zero and assuming that the two constitutive parameters controlling the rotational hardening, μ and β, are null. This approach will be employed in this work to compare the CPTu response for isotropic and anisotropic materials.

3. Numerical approach and constitutive parameters

In this work, analyses are carried out by means of G-PFEM (Geotechnical Particle Finite Element Method). G-PFEM is a computational framework tailored for analyzing large deformation problems in geomechanics, particularly focusing on insertion problems involving contacts. The methodology has been described in detail in previous works (Carbonell et al. 2022; Monforte et al. 2021). For use in G-PFEM the S-CLAY1 model was implemented using its generalization to three-dimensional stress conditions (Wheeler et al. 2003) extended to the finite strains regime, in which the deformation gradient decomposes multiplicatively in an elastic and plastic part.

Fully coupled hydromechanical simulations were conducted in an axisymmetric domain to model the penetration of a cone with standard dimensions and velocity (D=37.5mm, v=2cm/s). The domain, along with the boundary conditions of the axisymmetric model and the cone measurement positions, can be seen in Fig. 3. The domain is rectangular, with a width of $30R$ (r-axis). and a height of $60R$ (z-axis). The axis of symmetry is impervious, while the drainage was permitted in the rest of the boundaries. Null displacements are prescribed at the bottom boundary, whereas null radial displacements are prescribed at the vertical boundaries. At the top boundary, a vertical load was prescribed. A frictional cone/soil interface was adopted with a value of 15º.

3.1. Material characterization

Table 1 reports the employed constitutive parameters, which are thought to be representative of a normally consolidated, soft clay. For the anisotropic material, the initial fabric and the constitutive parameter of the rotational hardening law have been obtained using the equations proposed by Wheeler et al. (2003) for normally consolidated clays. The initial stress conditions correspond to p'=73kPa, q=40kPa, OCR=1.1, which corresponds to a K_0 = 0.58, computed according to the Jaky's formula.

Note that the initial stress state and constitutive parameters employed in these element tests are the same that will be employed for the simulations of CPTu.

To characterize the constitutive response of the soil, Fig. 1(a) reports the material response during undrained triaxial loading, considering both compression and extension tests. Two different materials are considered: one is isotropic (i.e. the Modified Cam Clay model) and the other is anisotropic. In these tests, deviatoric stress is applied or lowered parallel to the principal axis of the fabric.

The shape of the yield surface and the rotational hardening law produces a different stress path for the isotropic and anisotropic material, especially in the simulation of extension triaxial loading. In the simulation of undrained triaxial extension loading for the anisotropic

material, the material yields at a deviatoric stress in the range of a few kPa, then the stress path tends to the critical state line and finally reaches critical state at a similar mean effective stress and deviatoric stress than the isotropic material. In both the isotropic and anisotropic material materials, however, the value of the compression and extension undrained shear strengths is quite similar. Moreover, both materials predict the same ratio between the undrained shear strength for compression and extension conditions, since a Mohr Coulomb yield surface is employed to describe the Critical State surface at the stress space.

Figure 1(b) reports the evolution of the deviatoric stress in terms of the axial strain. For triaxial compression conditions, the constitutive response is quite similar, but the anisotropic material yields at a slightly higher stress and then presents a very reduced strain-softening. Differences are evident in the simulation of triaxial extension: both materials have the same strength, but the anisotropic material presents a lower stiffness.

The evolution of fabric is shown in Figure 1(c). Of course, fabric is always null for the isotropic material. In the other material, once the soil yields, fabric starts evolving. For triaxial compression loading, fabric increases from the initial value ($\alpha = 0.31$) to $\alpha = 0.33$, which coincides with $\frac{M_c}{3}$ for triaxial compression conditions. The same happens in the triaxial extension test, in which fabric tends to $\alpha = -0.25 = \frac{M_e}{3}$.

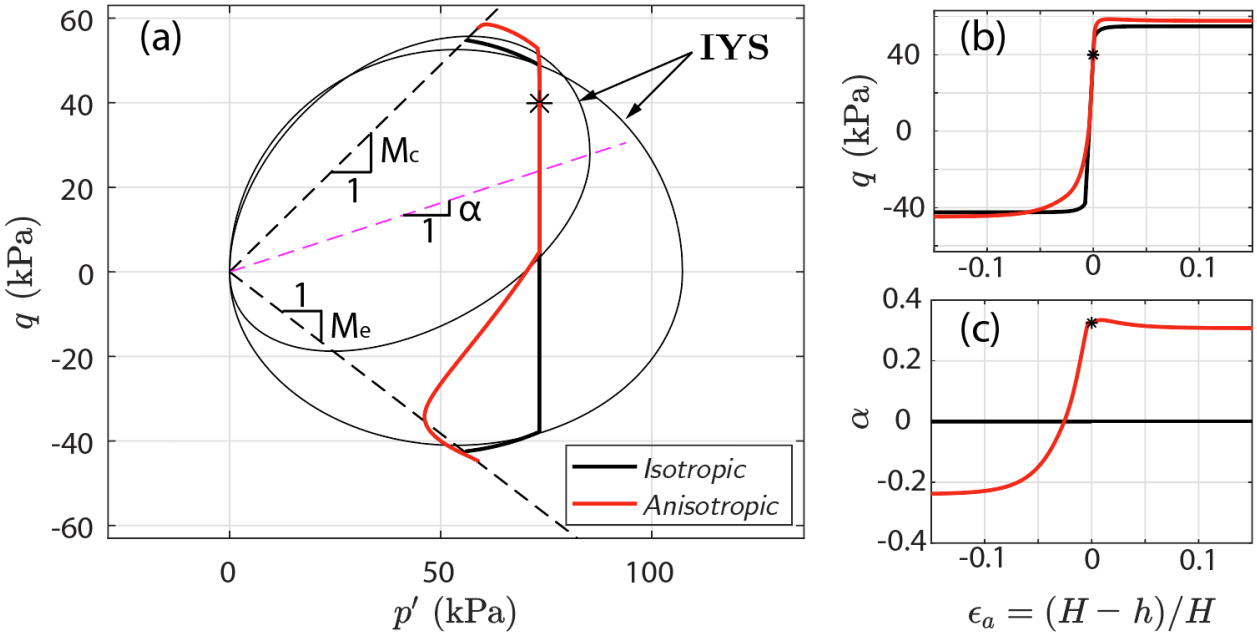

Figure 1. Stress paths for Triaxial Compression and triaxial extension of a lightly overconsolidated soil assuming isotropic and anisotropic behavior. Stress path on the mean effective stress, p', deviatoric stress, q, plane (a), evolution of deviatoric stress in terms of the axial deformation, (b), and evolution of fabric in terms of the axial strain, (c). IYS: initial yield surface, M_c: critical state line in compression, M_e: critical state line in extension, α: fabric.

4. Numerical results and discussion

In this section, we report the numerical results of CPTu testing in the two materials previously described. The permeability has been set to $k = 10^{-9}$ m/s. By doing this the material response is practically undrained.

Table 1. SCLAY-1 model parameters.

Material	α	μ	β
Isotropic	0	0	0
Anisotropic	0.31	67	0.5

SCLAY-1 parameters common to all materials: φ'=25°, κ=0.021, λ=0.168, ν=0.3, e_0=1.0

Fig. 2 reports the evolution of cone metrics in terms of the penetration. The net cone resistance and excess pore pressure at the face of the cone is slightly larger for the isotropic material with respect to the anisotropic material (see Table 2). On the other hand, the difference in excess pore pressure at the more conventional u_2 measuring position (cone shoulder) is minimal. The friction sleeve resistance seems also independent of the constitutive response of the soil. This may be expected, given that excess pore pressure is equalized at the shoulder and both materials share a unique friction angle at the soil-steel interface.

Table 2. Mean values of the results of CPTu simulations.

Material	q_{net} (kPa)	Δu_1 (kPa)	Δu_2 (kPa)	f_s (kPa)
Isotropic	297	268	186	20
Anisotropic	291	255	182	20

Contour plots of the excess water pressure are shown in Figure 3. The effect of anisotropy on the pore pressure field around the cone is small, although the size of the

bulb of high excess water pressure appears to be slightly larger for the isotropic material.

To characterize the material response during CPTu testing, Fig. 4(a) reports the stress path of a soil element initially located at a relative depth of $11R$ from initial position of the cone and at a radial distance of $1.15R$ from the symmetry axis whereas Fig. 4(b) plots the evolution of stress invariants and water pressure with respect to the relative distance of the tip of the cone with respect to this point.

From the initial stress state (relative distance $z = 11R$) up to a relative distance of around $7.5R$, the soil deforms elasto-plastically while approaching critical state (thus, the mean effective stress decreases, the deviatoric stress increases); water pressure variation is almost null. As the penetration of the CPTu progresses, the effective stress state does not suffer major changes. Additionally, the Lode's angle during the whole stress path is -30º (triaxial compression conditions). One aspect not shown in the figure is that in the simulation in which the soil response is anisotropic the orientation of the major fabric principal stress rotates until is almost parallel to the major effective stress (slight increase of the deviatoric stress).

Therefore, in both simulations, the stress path of this representative soil element is similar to the one that would result from undrained triaxial compression of a soil along the major principal direction of the fabric tensor. Although more simulations and analyses need to be done, this result could indicate that the governing undrained shear strength is the anisotropically consolidated, compression undrained shear strength.

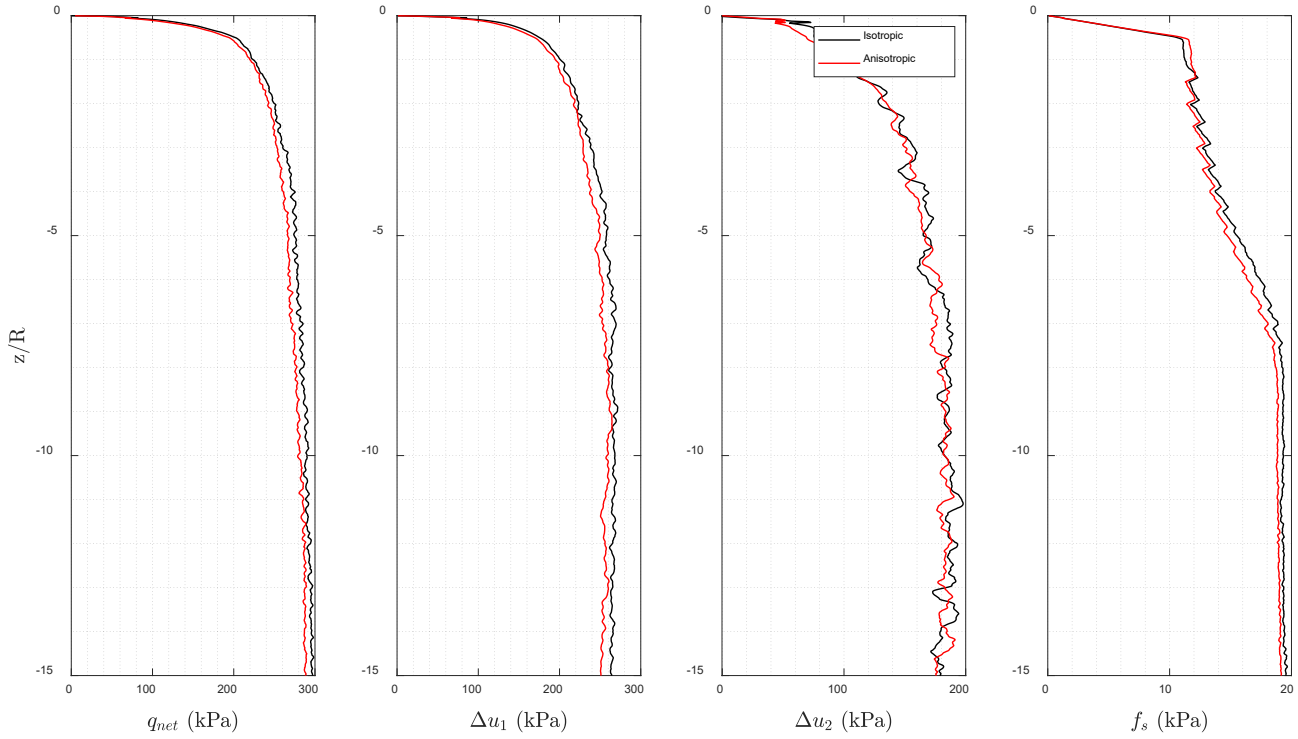

Figure 2. Results of the simulations of the CPTu tests φ' = 25º, *OCR*=1.1. Isotropic and anisotropic soil. Interface friction angle: 15º.

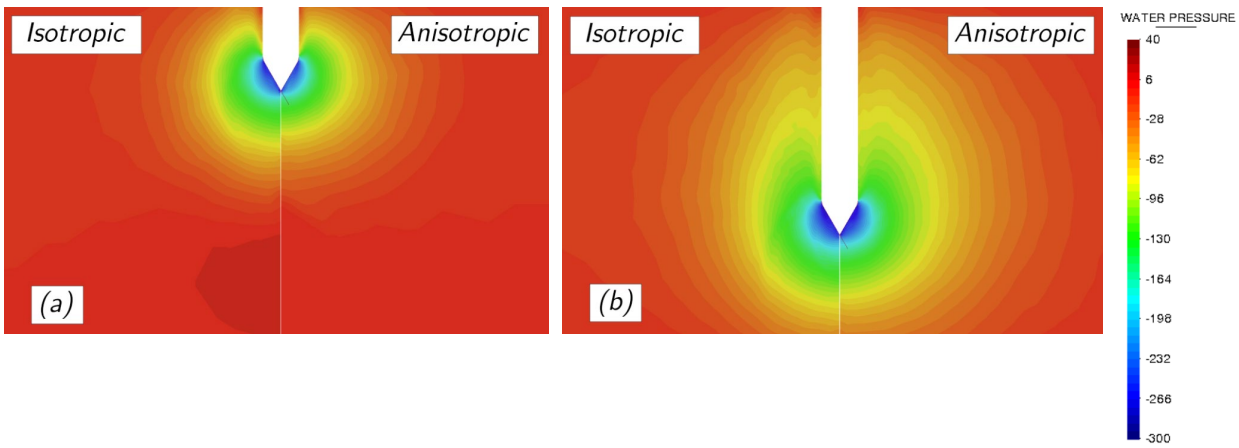

Figure 3. Contour plots of the excess water pressure after a penetration of $4R$ (a), $12R$ (b).

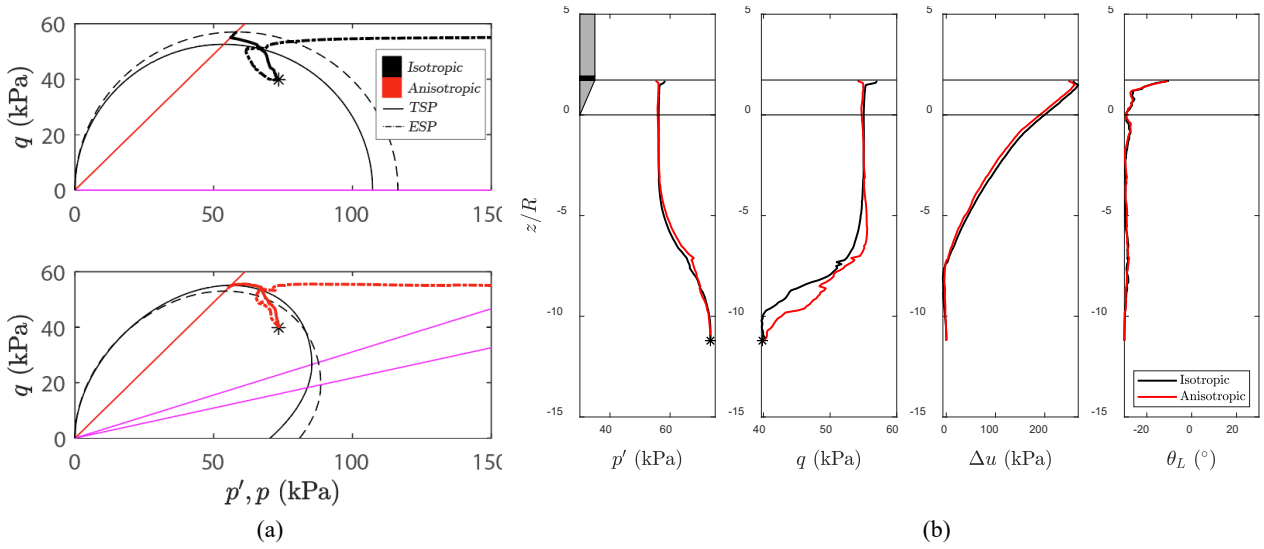

Figure 4. Stresses during cone penetration for a soil element initially located 1.15R from the axis for isotropic and anisotropic soil. φ'=25º. OCR=1.1. (a) Effective stress path (ESP) and total stress path (TSP) in p-q plane. (b) Variation of mean effective stress (p'), deviator stress (q), excess pore pressure (Δu) and Lode's angle (θ_L).

5. Conclusions

This work has been set out to investigate the effect of soil anisotropy on the CPTu response employing advanced numerical techniques.

We have reported the numerical analysis of CPTu in two distinct materials, with identical compression and extension undrained shear strength (as sheared along the principal axis of fabric), but one is isotropic and the other anisotropic.

The numerical results indicate a negligible impact of soil anisotropy during CPTu testing. Consequently, detecting anisotropy using CPTu appears challenging. Nevertheless, further research is necessary to confirm these conclusions.

Acknowledgements

The authors express their gratitude to Dr Laurin Hauser (CIMNE) for valuable suggestions and insights.

The authors gratefully acknowledge financial support of Ministerio de Ciencia, Innovación y Universidades of Spain (MCIN/AEI/10.13039/501100011033) through research grant PID2020-119598RB-I00.

References

Arroyo, M., & Muir-Wood, D. "Simplifications related to dynamic measurements of anisotropic G_0". In: Proc. Int. Symp. Deformation Characteristics of Geomaterials, Lyon, France, 2003.

Carbonell, J. M., Monforte, L., Ciantia, M, Arroyo, M., Gens, A. "Geotechnical Particle Finite Element Method for Modeling of Soil-Structure Interaction under Large Deformation Conditions." J Rock Mech, 14(3), pp. 967-983, 2022. https://doi.org/10.1016/j.jrmge.2021.12.006.

Isaksson, I., Karlsson, M., Dijkstra, J. "Modelling pile installation in soft natural clays". In: NUMGE 2023 (10th European Conf. on Numerical Methods in Geotech. Eng.), London, UK, 2023. https://doi.org/10.53243/NUMGE2023-48.

Kirkgard, M.M., Lade, P.V. "Anisotropy of Normally Consolidated San Francisco Bay Mud." Geotechnical Testing Journal 14.3: 231, 1991. https://doi.org/10.1520/GTJ10568J.

Low, H.E., Lunne, T., Andersen, K.H. Sjursen, M.A., Li, X., Randolph, M.F. "Estimation of Intact and Remoulded Undrained Shear Strengths from Penetration Tests in Soft Clays." Géotechnique 60(11), pp 843–59, 2010. https://doi.org/10.1680/geot.9.P.017.

Monforte, L., Gens, A., Arroyo, M., Mánica, M., Carbonell, J.M. "Analysis of Cone Penetration in Brittle Liquefiable Soils", Comput Geotech 134: 104123, 2021. https://doi.org/10.1016/j.compgeo.2021.104123.

Monforte, L., Arroyo, M., Gens, A. "Undrained strength from CPTu in brittle soils: A numerical perspective". In Cone Penetration Testing 2022 (pp. 591-597). CRC Press. https://doi.org/10.1201/9781003308829

Moug, D.M., Boulanger, R.W., DeJong, J.T., Jaeger, R.A. "Axisymmetric simulations of cone penetration in saturated clay". J. Geotech. Geoenviron. Eng, 145(4), 04019008, 2019. https://doi.org/10.1061/(ASCE)GT.1943-5606.0002024.

Su, S.-F. "Undrained Shear Strengths of Clay around an Advancing Cone", Can Geotech J, 47(10), pp. 1149–58, 2010. https://doi.org/10.1139/T10-011.

Su, S.F., Liao, H.J. "Effect of Strength Anisotropy on Undrained Slope Stability in Clay." Géotechnique 49 (2), pp. 215–30, 1999. https://doi.org/10.1680/geot.1999.49.2.215.

Wheeler, S.J., Näätänen, A., Karstunen, M., Lojander, M. "An Anisotropic Elastoplastic Model for Soft Clays." Can Geotech J 40(2): pp. 403–18, 2003. https://doi.org/10.1139/t02-119.

Wood, D. M. "Soil Behaviour and Critical State Soil Mechanics". Cambridge University Press, UK, 1990. https://doi.org/10.1017/CBO9781139878272.